# Application of the Koutecký-Levich Method to the Analysis of Steady State Voltammograms with Ultramicroelectrodes

Jiyeon Kim and Allen J. Bard*

Center for Electrochemistry, Department of Chemistry, The University of Texas at Austin, Austin, Texas 78712, United States

S *Supporting Information*

ABSTRACT: We demonstrate a new experimental approach to measure heterogeneous electron transfer rates. We adapted the classical Koutecký-Levich model for a rotating disk electrode (RDE) to a general heterogeneous electrochemical kinetic study with ultramicroelectrodes (UMEs) even for fast redox systems, where different sizes of UMEs are used to modulate the mass transfer rate (m). Subsequently, a linear plot of (1/current density) vs $1/m$ at different potentials can be created from the obtained steady state voltammograms, which is analogous to the traditional Koutecký-Levich plot. A simple numerical treatment with a slope and y-intercept from a linear plot allows for extracting kinetic parameters. A unifying treatment is presented for the steady state quasi-reversible, irreversible, and reversible voltammograms for a simple electron transfer reaction at UMEs. This new experimental approach with submicrometer to ~micrometer sized UMEs exceeds the mass transfer rates achieved by conventional electrochemical methods using rotating electrodes or solely tens of micrometer sized electrodes, thus enables us to study much faster heterogeneous electron transfer kinetics with simple instrumentation. The method should be particularly useful in studying particle size and structure effects.

$$\frac{1}{j} = \frac{1}{j_{mt}} + \frac{1}{j_{et}}$$
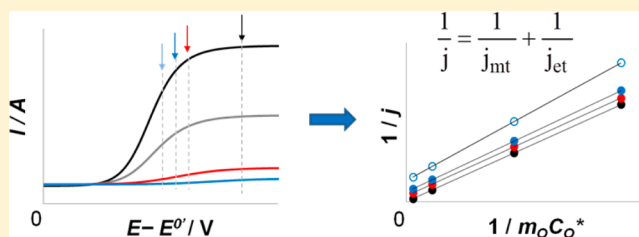
Since the introduction of ultramicroelectrodes (UMEs) in the 1990s, the use of steady-state voltammetry has been one of the most popular techniques for studying fast electrochemical kinetics compared to transient methods, because of several important advantages such as small charging current, negligible ohmic potential drop, simple data acquisition, and high reproducibility and accuracy.[1,2] The relatively simple theory of steady state technique and insensitivity to adsorption are also appealing compared to transient ones.

With interest in steady state voltammetry, there have been many studies to provide a simple analysis for estimating kinetic parameters, i.e., standard rate constant, k^0, and the transfer coefficient, α, from a steady state voltammogram. Oldham et al. proposed a simple analytical expression for a steady state voltammograms at a UME for both a disk and a hemisphere geometries.[3,4] Mirkin and Bard adapted the previous model using two quartile potentials and an experimental half wave potential and simplified them for the heterogeneous ET reaction as a quick and convenient experimental approach. This simple method, however, is susceptible to experimental artifacts, e.g., uncompensated resistive drop, and could affect the precise extraction of quartile potentials, thus resulting in over or underestimation of k^0 and α in this analysis. Mirkin and Amemiya have since proposed a new approach with a constraint by using paired voltammograms, which eliminate large uncertainties in kinetic parameters.[5,6] Paired voltammograms can be used with ion transfer at pipet-supported liquid/liquid interfaces or oxidation/reduction of both reduced and oxidized redox mediators in the bulk solution for a solid UME. Only a reduced (or oxidized) mediator is needed in the bulk

solution for a UME in the scanning electrochemical microscope (SECM) setup, where an oxidized (or reduced) mediator can be electrochemically generated by a macroscopic substrate.[7]

Here, we provide a quick and easy analysis method for irreversible to a nearly reversible case in heterogeneous electron transfer reactions using simple instrumentation, revisiting the classical Koutecký-Levich approach and demonstrating application to steady state voltammograms with different size UMEs. The Koutecký-Levich (K-L) model is widely used to analyze steady state voltammograms at the RDE, where the rotation rate or angular velocity is varied to adjust the mass transfer coefficient, m.[1,8] Instead, we vary the size of the UMEs for varying m and subsequently create a linear plot of 1/current density (j) vs $1/m$ at different potentials from the obtained steady state voltammograms, which is analogous to a traditional K-L plot. A unifying treatment is presented with covering the steady state quasi-reversible, irreversible, and reversible voltammograms for a simple electron transfer (ET) reaction at UMEs. The simplified analytical treatment is confirmed theoretically by using finite element simulation. We also apply the proposed model to a real electrochemical system to experimentally obtain the kinetic parameters. The range of applicability of the present method to heterogeneous kinetics and the improvement of its upper limits are discussed.

■ THEORY

We consider a generic one step electrochemical reaction

$$O + ne^- \underset{k_b}{\overset{k_f}{\rightleftharpoons}} R \tag{1}$$

where a redox mediator O is reduced to R at a UME. In this case, the steady-state current is governed by the rates of two competitive processes. (a) The mass transfer of O species from the bulk solution to near a UME surface. (b) The ET from the UME surface to species, O.

Depending on the rate of the ET reaction, the overall electrochemical reaction is categorized by reversible (Nernstian), quasi-reversible, and irreversible reactions.[1] Here, we treat the overall process as a sum of the reciprocals of the two competing processes of mass transfer and ET, so that the total current density, j, can be expressed as[9]

$$\frac{1}{j} = \frac{1}{j_{mt}} + \frac{1}{j_{et}} \tag{2}$$

where j_{et} and j_{mt} are the limiting current densities for heterogeneous kinetics at a UME surface and mass transfer of O to a UME surface, respectively. A mass transfer limited current density, j_{mt} can be written as

$$j_{mt} = Fm_O C_O^* \tag{3}$$

where F is the Faraday constant, C_O^* is the bulk concentration of O in solution. m_O is a mass transfer coefficient, expressed in terms of the size and the shape of UMEs, e.g., $m_O = 4D_O/\pi r_0$ for a disk UME, $m_O = D_O/r_0$ for a spherical electrode, where r_0 is the radius of each geometry and D_O is a diffusion coefficient of the O species, which is well-known from the theory of UMEs.[1]

Here, we use the Butler−Volmer model to treat heterogeneous kinetic currents and assume $n = 1$. The steady state current density for a quasi-reversible case is expressed as[1]

$$j = F(k_f C_{O(y=0)} - k_b C_{R(y=0)}) \tag{4}$$

By defining the exchange current density,

$$j_0 = Fk^0 C_O^* e^{-\alpha F/RT(E_{eq}-E^{0'})} = Fk^0 C_O^{*1-\alpha} C_R^{*\alpha}$$

with

$$b = e^{F/RT(E-E_{eq})}$$

and

$$E_{eq} = E^{0'} + \frac{RT}{F}\ln\left(\frac{C_O^*}{C_R^*}\right)$$

Rearranging eq 4 yields

$$\frac{1}{j} = \frac{1}{FmC^*}\left(\frac{1+pqb}{1-b}\right) + \frac{1}{Fk^0 C^*}\frac{(pb)^\alpha}{(1-b)} \tag{5}$$

where $C^* = C_O^*$, the concentration ratio, C_O^*/C_R^* is p, $m_O = m$, and the mass transfer coefficient ratio, m_O/m_R is q. The resulting eq 5 is directly analogous to eq 2 including the contribution of the kinetic and the mass transfer terms, and thus a similar form to the K-L relationship (detailed derivation is in the Supporting Information).

Subsequently, a linear plot with a slope

$$\frac{(1+pqb)}{F(1-b)}$$

can be obtained if $1/j$ is plotted against $1/mC^*$. An extrapolation to $1/(mC^*) \rightarrow 0$ allows for the determination of kinetic parameters for the electron transfer reaction from the y-intercept,

$$\frac{1}{Fk^0 C^*}\frac{(pb)^\alpha}{(1-b)}$$

Especially, in the range of potential, $E - E^{0'} \leq -60$ mV, a constant slope of $1/F$ is expected from obtained linear plots due to a negligibly small b (detailed information is in the Supporting Information, Table S1). Resultantly, parallel linear plots with different y-intercepts can be yielded at different potentials in the given range. In that sense, our approach for a quasi-reversible case would be more adaptable in the potential range of $E - E^{0'} \leq -60$ mV for one electron reduction reaction, where a slope of a linear plot maintains $1/F$ independent with applied E. Similarly, the applicable potential range as $E - E^{0'} \geq 40$ to 60 mV could be derived for a quasi-reversible oxidation reaction with one step, one electron transfer; and more detailed information can be found in the Supporting Information. Noticeably, in either quasi-reversible reduction or oxidation reaction, $m_R \neq m_O$ does not influence a y-intercept implying no effect on the overall kinetic analysis.

We further confirmed our theoretical approach by finite element analysis with COMSOL MULTIPHYSICS v 4.2a. Voltammograms were simulated for one step, one electron reduction of oxidized species, O, where $E^{0'}$, C_O^*, C_R^*, E_{eq} and α are 0.3 V, 1 mM, 0.01 mM, 0.42 V, and 0.5, respectively for Pt disk UMEs with a radii of 150 nm, 600 nm, 2.5 μm, and 5 μm. Diffusion coefficients, D of oxidized and reduced redox molecules were assumed to be the same as 7.4×10^{-6} cm²/s. k^0 ranges from 4×10^{-4} to 4 cm/s to represent irreversible, quasi-reversible, and reversible cases. For a quasi-reversible reaction with $k^0 = 0.04$ cm/s, a set of voltammograms are simulated with various radii of Pt disk as presented in Figure 1a. The respective steady state currents normalize currents to show differences in curve shapes. Clearly, the half wave potential, $E_{1/2}$, is shifted by 80 mV as the electrodes become smaller, from 5 μm to 150 nm. Such a sluggish current response for smaller electrodes results from more kinetically limited electron transfer due to more efficient mass transfer. Current densities (j) at different potentials, e.g., $E - E^{0'} = -0.41$, -0.11, -0.08, and -0.04 V were chosen to subsequently plot $1/j$ vs $1/(m_O C_O^*)$ presented in Figure 1b. At $E - E^{0'} = -0.41$ V, the electrochemical reaction is primarily governed by mass transfer, so that a plot of $1/j$ intersects the origin. As expected, a less cathodic potential leads to a larger y-intercept in the plot of $1/j$ vs $1/(m_O C_O^*)$.

A fairly fast quasi-reversible case of one-electron reduction reactions with k^0 0.4 cm/s was also studied. In this case, we simulated steady state voltammograms with the radii of Pt UME from 50 nm, 70 nm, 150 nm, 600 nm, 2.5 μm, and 5 μm in Figure 2a. As the size of Pt UME gets smaller, the voltammogram becomes more sluggish indicating that the ET reaction is more kinetically limited at the higher current density. A series of plots of $1/j$ vs $1/(m_O C_O^*)$ was created from voltammograms with radii of 150 nm, 600 nm, 2.5 μm, and 5
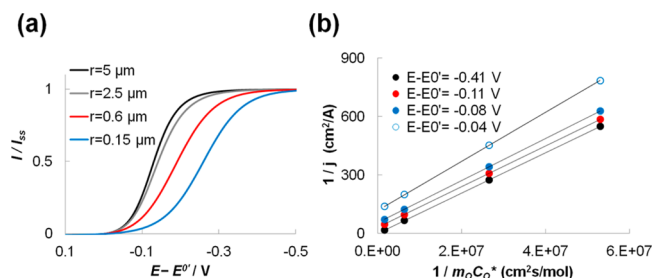
Figure 1. (a) Simulated steady state voltammograms by COMSOL MUTIPHYSICS v.4.2 for a quasi-reversible one electron reduction reaction, where $E^{0'}$, k^0, C_O^*, C_R^*, E_{eq}, and α are 0.3 V, 0.04 cm/s, 1 mM, 0.01 mM, 0.42 V, and 0.5, respectively, with various radii of Pt disk UMEs, 150 nm, 600 nm, 2.5 μm, and 5 μm. Diffusion coefficient and concentration of O species are 7.4×10^{-6} cm²/s and 1 mM, thus m_O = 0.019, 0.038, 0.16, and 0.63 cm/s, respectively. All currents are normalized by their respective steady state currents. (b) Set of linear plots of $1/j$ vs $1/m_O C_O^*$ obtained from voltammograms in part a at potentials $E - E^{0'}$ = −0.41, −0.11, −0.08, −0.04 V. At $E - E^{0'}$ = −0.41 V, the overall reaction is mainly governed by the mass transfer, thus a plot of $1/j$ intersects the origin. A less cathodic potential brought a larger y-intercept in these linear plots.

μm Pt UMEs at given potentials, $E - E^{0'} \leq -60$ mV. These plots show a linearity maintaining the constant slope as $1/F$ with different y-intercepts in Figure 2b. Since k^0 is large, the y-intercepts only show a slight deviation from the origin at the given potentials, $E - E^{0'} \leq -60$ mV compared to the slower k^0 (see Figure 2b and Figure S2b). These y-intercepts, however,

are measurable to yield the kinetic information shown in the inset of Figure 2b.

For fast quasi-reversible electrode reactions, the available potential range in the present method is quite narrow because of the constraint of $E - E^{0'} \leq -60$ mV for a constant slope, $1/F$, while $|E - E^{0'}|$ should be less than the total mass transfer controlled regime, thus still showing the significant deviation of the y-intercept from the origin. In this regard, a smaller UME is advantageous to expand the available potential range as the electrochemical reaction at small UME is more kinetically controlled due to highly enhanced mass transfer rate (m). For example, in Figure 2a, the currents at a 50 nm or a 70 nm Pt UME at a sufficiently large cathodic potential, e.g., $E - E^{0'}$ = −150 to −200 mV are still deviated from the steady state current controlled by the mass transfer compared to 2.5 and 5 μm radius Pt UMEs. Thereby, a discernibly significant deviation of the y-intercept from the origin can be obtained in a plot of $1/j$ vs $1/(m_O C_O^*)$ even at $E - E^{0'}$ = −150 mV, which enables us to reliably extract kinetic information for a fast ET reaction. In Figure 2c, $1/j$ vs $1/(m_O C_O^*)$ is plotted with smaller UMEs of 50, 70, and 150 nm radii, where the clear deviation of y-intercept from the origin is found in the wide range of $E - E^{0'}$ = −80 to ∼−160 mV compared to $E - E^{0'}$ = −80 to −100 mV in Figure 2b. This result clearly presents the advantage of small UMEs in the fast ET kinetic study. In Figure 2b,c, a slope of $1/F$ starts to deviate when $E - E^{0'}$ > −60 mV as predicted.
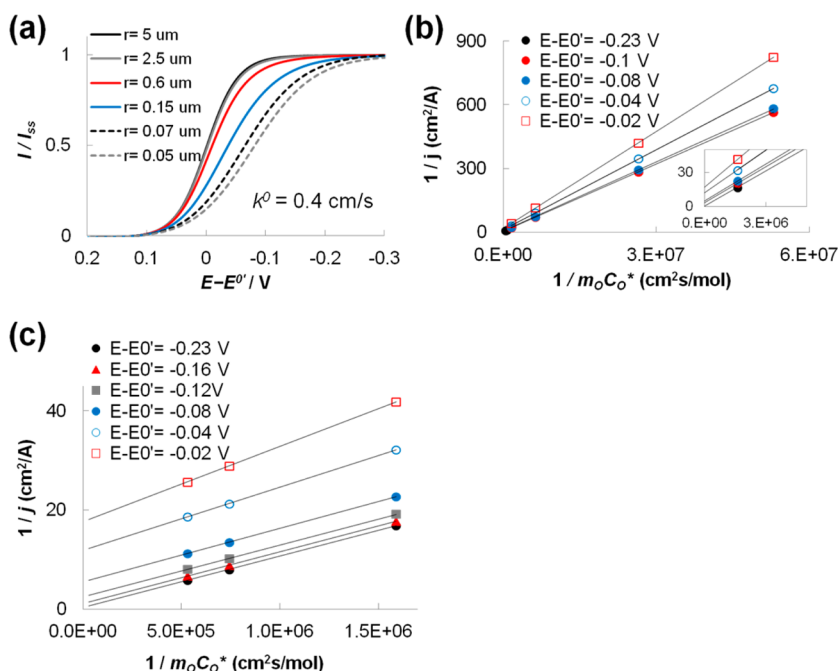

Figure 2. (a) Simulated steady state voltammogram for a quasi-reversible one electron reduction reaction with k^0 = 0.4 cm/s, where $E^{0'}$, C_O^*, C_R^*, E_{eq} and α are 0.3 V, 1 mM, 0.01 mM, 0.42 V, and 0.5, respectively, with various radii of Pt disk UMEs, 50 nm, 70 nm, 150 nm, 600 nm, 2.5 μm, and 5 μm. More kinetically limited voltammograms at smaller Pt UMEs are seen due to higher mass transfer rate. Their respective steady state currents normalize all currents in voltammograms. (b) Corresponding plots of $1/j$ vs $1/m_O C_O^*$ at various given potentials from voltammograms with 150 nm to ∼5 μm radius Pt UMEs in part a. A slope of all lines is constantly $1/F$ in the range of $E - E^{0'} \leq -60$ mV. In the magnified plot of an inset, the y-intercepts at each given potential are shown. (c) Plot of $1/j$ vs $1/m_O C_O^*$ corresponding to the radii of Pt disk UMEs 50 nm, 70 nm, and 150 nm. Because of more kinetically limited voltammograms with smaller Pt UME, wider potential ranges are available for a significant deviation of y-intercepts from the origin before reaching a mass transfer limit, i.e., y-intercept = 0.

Other cases of quasi-reversible reactions, a very slow or a very fast ET showing almost Nernstian behavior with $k^0 = 4 \times 10^{-4}$ cm/s or $k^0 = 4$ cm/s, respectively, were also studied in the Supporting Information. Irreversible and reversible ET cases were also discussed in the Supporting Information.

In conclusion, the simulation results are generally in agreement with the simpler steady-state treatment and it is possible to define the limits where the linear plots can be used to extract kinetic information about the electrode reaction.

■ EXPERIMENTAL SECTION

Chemicals. 1,1′-Ferrocenedimethanol (FcDM, 97%) was purchased from Sigma-Aldrich and recrystallized with hexane before doing the electrochemistry. Potassium nitrate (KNO$_3$, Fisher) was used as received without further purification. Ultra nanopure water with 18.2 MΩ cm resistivity and the 3 ppb TOC level (Milli-Q integral 5 system, EMD Millipore Corporation) was used for all solution preparation.

Instrumentation. The electrochemical measurements were performed using a CHI model 920C potentiostat (CH Instruments, Austin, TX) with the two-electrode cell placed in the grounded stage. Ag/AgCl in a saturated KCl solution was used as a reference and counter electrode. The SEM image of Pt electrodes was obtained using the dual beam instrument (FEI Strata DB235 dual beam SEM/FIB) (Figure 3). To avoid
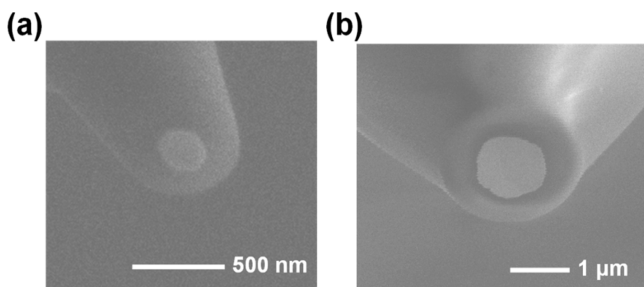
Figure 3. SEM images of FIB milled Pt UMEs with radii of (a) 90 nm and (b) 0.6 μm.

the electrostatic damage on the electrode surface, we followed the method of the electrostatic damage (ESD) protection reported by Amemiya et al.[10] With all the ESD damage protection, the measurement of the cyclic voltammetry was carried out in a humidity controlled room with higher than 30% relative humidity at 20 °C.

Preparation of Pt UMEs. The Pt UMEs were prepared according to a procedure reported elsewhere by laser pulling (Sutter Instruments) followed by milling with a focused ion beam (FEI Strata DB235 dual beam SEM/FIB).[11] The radius of the Pt UME was checked electrochemically by cyclic voltammetry in 1 mM FcDM, 0.5 M KNO$_3$ solution, which was consistent with that measured by SEM.

■ RESULT AND DISCUSSION

We experimentally confirmed this theoretical approach by studying the heterogeneous ET reaction of 1,1′-ferrocenedimethanol (FcDM) with Pt UMEs of varying sizes. FcDM undergoes a one step, one-electron oxidation reaction, which is well-known to be a fast quasi-reversible reaction. A series of cyclic voltammograms (CVs) at 20 mV/s with 1 mM FcDM in 0.5 M KNO$_3$ were obtained with Pt disk UMEs with radii of 90 nm, 600 nm, 1.9 μm, and 4.2 μm milled by a focused ion beam.

These radii of Pt UMEs were estimated using eq 6 from steady state currents in CVs, which were consistent with those observed by SEM (Figure 3).

$$i_{ss} = 4xnFD_R C_R^* r_0 \tag{6}$$

where x is 1.08, a coefficient for the RG value (the ratio between the radii of glass sheath and Pt),[10] $n = 1$, $D_R = 7.4 \times 10^{-6}$ cm^2/s, $C_R^* = 1.0$ mM, and r_0 is the electrode radius.

Normalized CVs are given in Figure 4a measured with various radii of Pt UMEs (solid lines), where $E^{0'}$ is 0.175 V vs Ag/AgCl. $E^{0'}$ was independently determined by CV at 20 mV/s with 25 μm diameter Pt UME (data not shown). Subsequently, $1/j$ vs $1/(m_R C_R^*)$ were plotted at given potentials of $E - E^{0'} = 0.045, 0.055, 0.075,$ and 0.175 V. A clear deviation of the resulting slope from $1/F$ was observed when $E - E^{0'} < 40$ mV. At $E - E^{0'} = 0.175$ V, the ET reaction is in mass transfer controlled regime, thus the plot of $1/j$ intersects the origin in Figure 4d. As the potential becomes smaller thus more kinetically limited, the y-intercept deviates more from the origin. From the y-intercepts at different potentials, we could estimate the heterogeneous standard electron transfer rate, $k^0 = 0.45 \pm 0.03$ cm/s when α is 0.5. Assumption of C_R^*/C_O^* ranging from 100 to 1000 as a realistic impurity level based on a nearly zero initial current in CV, thus E_{eq} being from 0.057 to -0.002 V does not impact the obtained rate constant. Using COMSOL MULTIPHYSICS v 4.2a, experimental CVs were further fitted with theoretical curves (open circles in Figure 4b,c). When k^0 is 0.45 cm/s with $\alpha = 0.5$, the best fit was obtained over all CVs for 90 nm, 600 nm, 1.9 μm, and 4.2 μm Pt UMEs as presented in Figure 4c. These kinetic parameters for FcDM are close to previously reported values.[12] Notably, the mass transfer rate, m_R for the radius 2.5 to 5 μm UMEs is 0.04 to 0.02 cm/s, respectively, with given D_R, which is slower than the electron transfer rate. Since k^0 already exceeds the m_R for upper sized UMEs among radii of 50 nm to 5 μm, the mass transfer dominates in this given system. This tells that the present approach is useful to extract kinetic information over a wide range of heterogeneous ET rates even in the system where the mass transfer contributes significantly.

In practice, it is useful to construct a plot of $1/j$ at UMEs with a wide range of sizes, especially when there is no prior knowledge about the kinetics for a given electrochemical reaction. In this case, for a reliable kinetic analysis, the current in voltammograms should deviate significantly, e.g., depending on the signal-to-noise ratio, at least ~1% from totally reversible voltammogram at $E - E^{0'} = -60$ mV in heterogeneous ET reduction reaction (or 60 mV for oxidation reaction). This constraint is applied to the largest size of UMEs and determines the upper limit of an applicable range of UME sizes for the K-L analysis. The deviation degree increases inversely proportionally to an UME size, thereby a 10 times smaller UME causes ~10% deviating current from the totally reversible voltammogram. An order of magnitude current deviation can yield data points widely spanning a region in a K-L plot, showing a characteristic linear K-L plot with a slope of $1/F$. Meantime, the minimum deviation of ~1% to more than 10% from variously sized UMEs can lead to a clearly significant kinetic effect compared to mass transfer control in a K-L plot, thus allowing for a reliable measurement of kinetic parameters. These ranges of current deviation are required as an upper limit of applicable
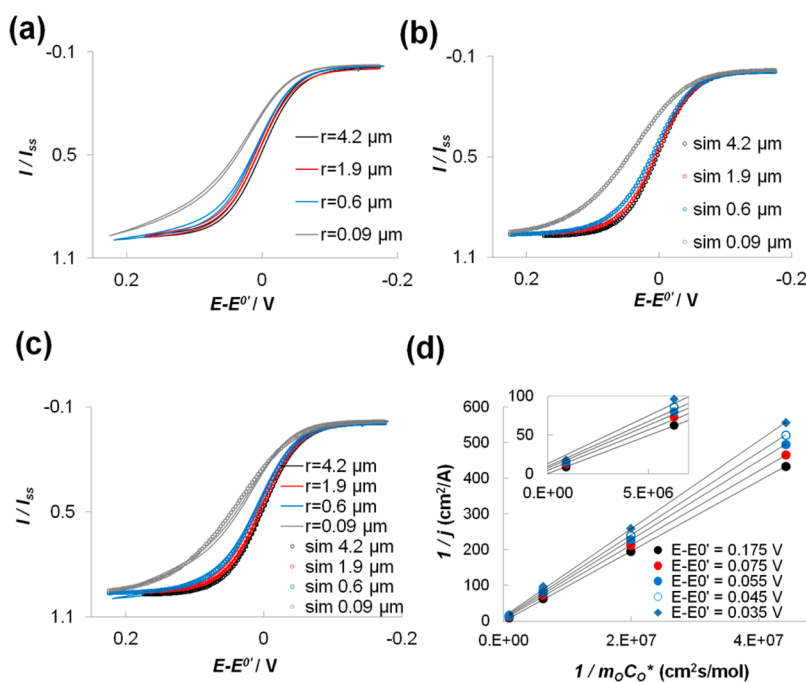
Figure 4. (a) Normalized CVs for the oxidation reaction of 1 mM FcDM in 0.5 M KNO$_3$ with 90 nm, 600 nm, 1.9 μm, and 4.2 μm Pt UMEs at 20 mV/s (solid lines). (b) Theoretical curves simulated with COMSOL MULTIPHYSICS v. 4.2 (open circles), where k^0 is 0.45 cm/s with α = 0.5. Each curve was normalized with the respective steady state current. (c) Each experimental curve was fit with theoretical curves. (d) Set of plots of $1/j$ vs $1/(m_R C_R^*)$ obtained from CVs (a) at $E - E^{0'}$ = 0.035, 0.045, 0.055, 0.075, and 0.175 V. The heterogeneous standard electron transfer rate, k^0 = 0.45 $\pm$ 0.03 cm/s, was determined with α = 0.5 from a set of y-intercepts at different given potentials. The inset magnified the plot showing the deviation of y-intercepts from the origin at different given potentials.

UME size for confidence in the kinetic analysis. Certainly, one can use any smaller size UME to see the kinetic effect more clearly in a given K-L plot (as in Figure 2c).

Often a rotating disk electrode (RDE) is used to obtain kinetic information. However, the RDE can have a maximum rotating velocity of 10 000 rpm equivalent to a mass transfer rate of ~0.05 cm/s assuming D = 7.4 × 10^{-6} cm^2/s, thus the measurable kinetic limit is smaller than 0.05 cm/s.[13] UMEs and scanning electrochemical microscopy (SECM) offer much higher mass transfer rates. In SECM, for example, a small gap of nm dimensions between the UME tip and the substrate can greatly enhance the mass transfer rate to measure fast kinetics as high as tens of cm/s.[7,14] Compared to these techniques, the UME approach described here is efficient enough to reliably measure a heterogeneous ET rate constant up to 1 cm/s with simple instrumentation, since only a series of micrometer to ~sub micrometer sized UMEs and a potentiostat are needed for a set of CVs. Moreover, a tunneling ultramicroelectrode (TUME) can achieve even smaller sizes, e.g. tens ~a few nanometer dimensions, since its dimension is determined by the size and the shape of nanoparticles. As a result, it can yield higher mass transfer rates. In that sense, the utilization of TUMEs in the present method will allow for reliable measurements of a fast heterogeneous ET rates up to tens of cm/s. An approach based on a disk UME is applicable to a spherical geometry of a TUME as well, since there is no difference between the two geometries under reversible kinetics and very little difference in voltammograms under irreversible conditions.[4,15] Table 1 presents mass transfer rates for a range of different radius of disk UMEs and equivalent rotating rates required to produce the same mass transfer rate in RDE experiments or equivalent scan rate for fast scan cyclic

Table 1. Comparisons of Mass Transfer Rates (m) for Disk UMEs of Different Radii and the Equivalent Rotation Rates (ω) Required to Produce the Same Mass Transfer Rate in a RDE Experiment, or the Equivalent Scan Rate (v) for Fast Scan Cyclic Voltammetry[a]

m/cm s^{-1}	UME radius, r/μm	ω/rpm	v/V s^{-1}
94.3	0.001	3.57 × 10^{10}	3 × 10^7
m	$\propto r^{-1}$	$\propto \sqrt{\omega}$	$\propto \sqrt{v}$
0.009	10	357	0.3

[a]Calculation assumed D = 7.4 × 10^{-6} cm^2/s and the kinematic viscosity of the electrolyte is v = 1.1 × 10^{-2} cm^2/s.

voltammetry.[1] Practically, the limitation of fast scan CVs at 3 × 10^7 V/s is obvious due to a high capacitive current compared to the faradaic current, distortion of voltammograms by uncompensated resistance, and the high susceptibility of adsorption.

In reality, we can think about two possibilities of the distortion in a K-L plot. One possibility may come from "the smallest current density" with the largest electrode, since the largest $1/j$ (i.e., the smallest current density) significantly affects the slope and y-intercept in the linear plot. In this case, the constraint of the slope, $1/F$ in the K-L plot can be used to evaluate whether the largest data point overwhelms the plot or not. The other possible scenario for distortion may result from "the largest current density" with the smallest electrode. As long as the electrodes have a reliably high quality in terms of geometry, this distortion could be used to evaluate the size effect on the given heterogeneous ET system. In these regards, the use of ~1 order of magnitude range of electrode radius will be adequate to have proportionate weight to each data point in

K-L analysis. Therefore, this new K-L method should be particularly useful in studying particle size and structure effects.

CONCLUSION

A new experimental approach has been demonstrated to extract kinetic information from different types of steady state voltammograms under nearly reversible, quasi-reversible, and irreversible conditions. We adapted the classical Koutecký-Levich model for a rotating disk electrode to a general electrochemical kinetic study even for a fast redox system, where different size UMEs are used to modulate the mass transfer rate. This new experimental approach is easy to use since it only needs different size UMEs for a series of steady state voltammograms. A subsequent plot of $1/j$ vs $1/mC*$ obtained at different potentials is used to measure the kinetic parameters of k^0 and α for the corresponding ET reaction from the slope and y-intercept. The validity of this method has been experimentally demonstrated by the electrochemical oxidation of FcDM. Notably, the proposed method with sub micrometer to ~tens of micrometer sized UMEs exceeds the mass transfer rates achieved by conventional electrochemical methods using rotating electrodes or solely tens of micrometer sized electrodes, thus enabling us to study much faster ET kinetics with simple instrumentation. The approach is applicable to not only inlaid disk but also spherical geometry such as a TUME with nanometer dimensions; thereby, the upper limit of this approach can be further improved up to tens of cm/s by employing TUMEs.

ASSOCIATED CONTENT

Ⓢ Supporting Information

The Supporting Information is available free of charge on the ACS Publications website at DOI: 10.1021/acs.analchem.5b03965.

Derivations, discussion of potential range for K-L analysis, and finite element simulations (PDF)

AUTHOR INFORMATION

Corresponding Author
*E-mail: ajbard@mail.utexas.edu.

Notes

The authors declare no competing financial interest.

ACKNOWLEDGMENTS

REFERENCES

(1) Bard, A. J.; Faulkner, L. R. *Electrochemical Methods*; Wiley: New York, 1980.
(2) Mirkin, M. V.; Bard, A. J. *Anal. Chem.* **1992**, *64*, 2293−2302.
(3) Oldham, K. B.; Myland, J. C.; Zoski, C. G.; Bond, A. M. *J. Electroanal. Chem. Interfacial Electrochem.* **1989**, *270*, 79.
(4) Oldham, K. B.; Zoski, C. G. *J. Electroanal. Chem. Interfacial Electrochem.* **1988**, *256*, 11−19.
(5) Rodgers, P. J.; Amemiya, S.; Wang, Y.; Mirkin, M. V. *Anal. Chem.* **2010**, *82*, 84−90.
(6) Wang, Y.; Velmurugan, J.; Mirkin, M. V.; Rodgers, P. J.; Kim, J.; Amemiya, S. *Anal. Chem.* **2010**, *82*, 77−83.
(7) Nioradze, N.; Kim, J.; Amemiya, S. *Anal. Chem.* **2011**, *83*, 828−835.
(8) Levich, V. G. *Physicochemical Hydrodynamics*; Prentice-Hall: Englewood Cliffs, NJ, 1962.
(9) Hill, C. M.; Kim, J.; Bard, A. J. *J. Am. Chem. Soc.* **2015**, *137*, 11321−11326.
(10) Nioradze, N.; Chen, R.; Kim, J.; Shen, M.; Santhosh, P.; Amemiya, S. *Anal. Chem.* **2013**, *85*, 6198−6202.
(11) Kim, J.; Izadyar, A.; Nioradze, N.; Amemiya, S. *J. Am. Chem. Soc.* **2013**, *135*, 2321−2329.
(12) Abbou, J.; Demaille, C.; Druet, M.; Moiroux, J. *Anal. Chem.* **2002**, *74*, 6355−6363.
(13) Chen, S.; Kucernak, A. *J. Phys. Chem. B* **2004**, *108*, 3262−3276.
(14) Sun, P.; Mirkin, M. V. *Anal. Chem.* **2006**, *78*, 6526−6534.
(15) Bond, A. M.; Oldham, K. B.; Zoski, C. *Anal. Chim. Acta* **1989**, *216*, 177−230.